H_2/D_2 separation in gas chromatography through a MOF-on-MOF strategy using γ-AlOOH@Al(OH)(1,4-NDC)@ZIF-67 as stationary phase via additive effects of chemical affinity quantum sieving and kinetic sieving

Enming Ping, Lingyun Kong, Mengyao Liu, Yunshan Zhou*, Lijuan Zhang*, Nan Chen

State Key Laboratory of Chemical Resource Engineering, College of Chemistry, Beijing University of Chemical Technology, Beijing 100029, P. R. China

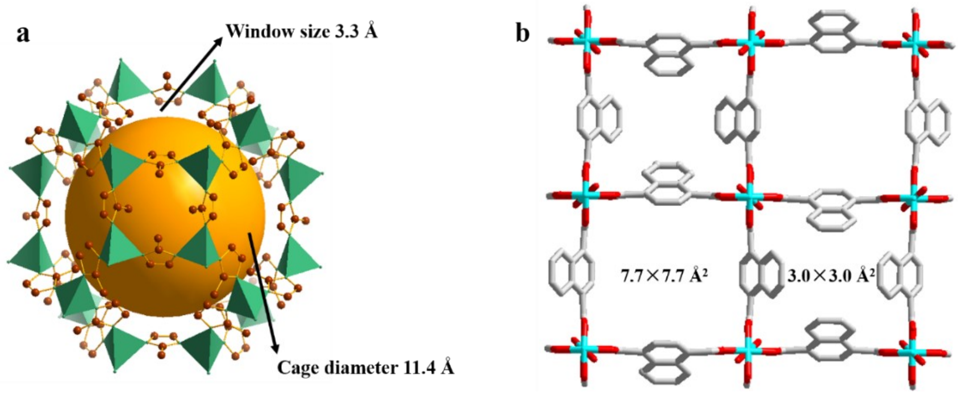

Fig. S1 The pore structure of ZIF-67 (the window size of 3.4 Å, the cage diameter of 11.4 Å) (a) and Al(OH)(1,4-NDC) (two types of pores, 7.7 × 7.7 $Å^2$ and 3.0×3.0 $Å^2$) (b).

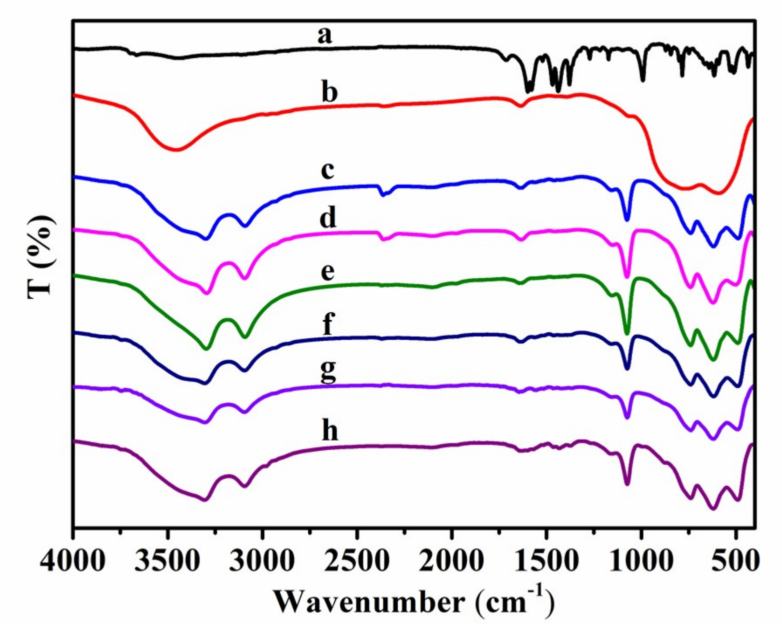

Fig. S2 IR spectra of Al(OH)(1,4-NDC) (line a), γ-Al_2O_3 (line b), γ-AlOOH (line c), γ-AlOOH@1.02%-Al(OH)(1,4-NDC) (line d), γ-AlOOH@1.12%-Al(OH)(1,4-NDC) (line e), γ-AlOOH@2.61%-Al(OH)(1,4-NDC) (line f), γ-AlOOH@4.35%-Al(OH)(1,4-NDC) (line g), γ-AlOOH@6.63%-Al(OH)(1,4-NDC) (line h).

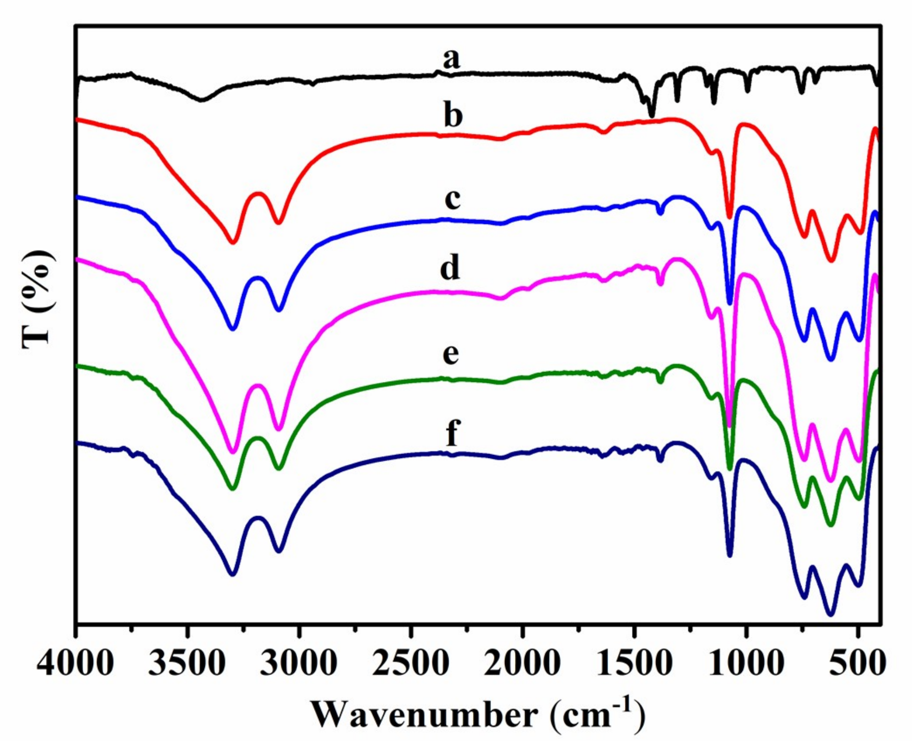

Fig. S3 IR spectra of ZIF-67 (line a); γ-AlOOH@1.12%-Al(OH)(1,4-NDC) (line b); γ-AlOOH @1.12%-Al(OH)(1,4-NDC)@1-ZIF-67 (line c); γ-AlOOH @1.12%-Al(OH)(1,4-NDC)@2-ZIF-67 (line d); γ-AlOOH @1.12%-Al(OH)(1,4-NDC)@3-ZIF-67 (line e); γ-AlOOH@1.12%-Al(OH)(1,4-NDC)@4-ZIF-67 (line f).

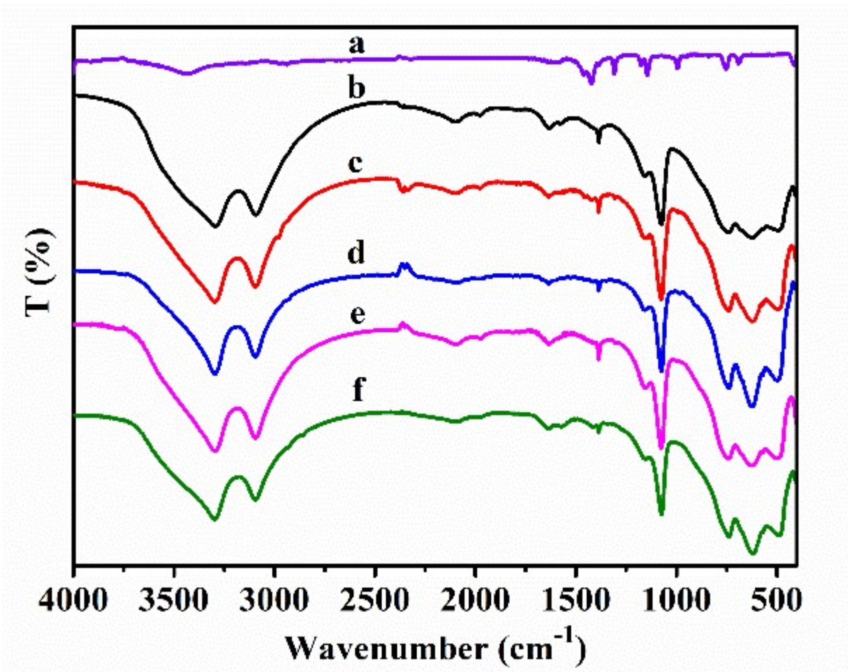

Fig. S4 IR spectra of ZIF-67 (line a); γ-AlOOH@2-ZIF-67 (line b); γ-AlOOH@4-ZIF-67 (line c); γ-AlOOH@6-ZIF-67 (line d); γ-AlOOH@8-ZIF-67 (line e); γ-AlOOH (line f).

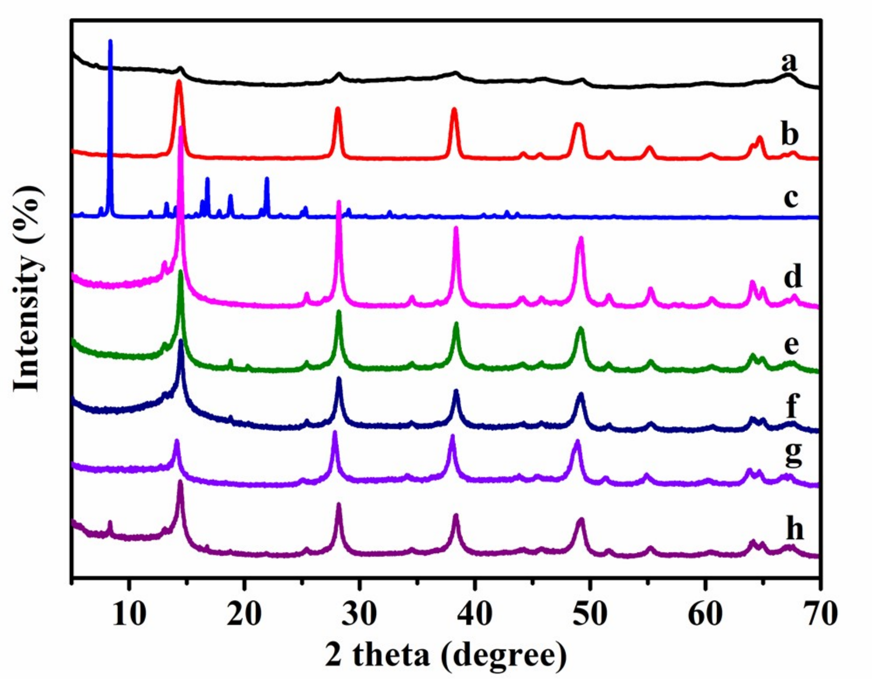

Fig. S5 P-XRD patterns of γ-Al_2O_3 (line a), γ-AlOOH (line b), Al(OH)(1,4-NDC) (line c), γ-AlOOH@1.02%-Al(OH)(1,4-NDC) (line d), γ-AlOOH@1.12%-Al(OH)(1,4-NDC) (line e), γ-AlOOH@2.61%-Al(OH)(1,4-NDC) (line f), γ-AlOOH@4.35%-Al(OH)(1,4-NDC) (line g), γ-AlOOH@6.63%-Al(OH)(1,4-NDC) (line h).

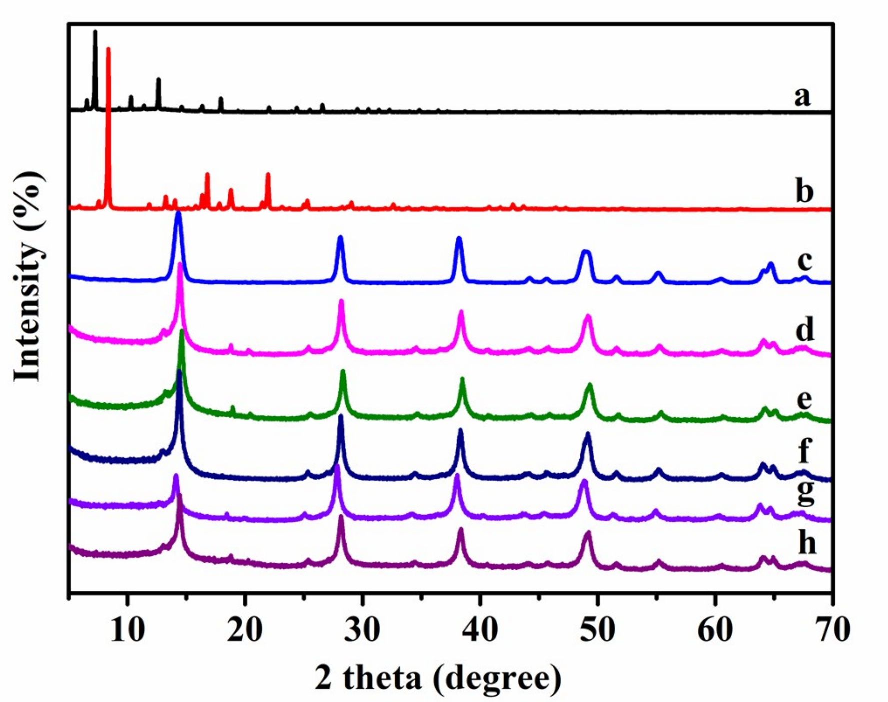

Fig. S6 P-XRD patterns of ZIF-67 (line a), Al(OH)(1,4-NDC) (line b), γ-AlOOH (line c), γ-AlOOH@1.12%-Al(OH)(1,4-NDC) (line d), γ-AlOOH@1.12%-Al(OH)(1,4-NDC)@1-ZIF-67 (line e), γ-AlOOH@1.12%-Al(OH)(1,4-NDC)@2-ZIF-67 (line f), γ-AlOOH@1.12%-Al(OH)(1,4-NDC)@3-ZIF-67 (line g), γ-AlOOH@1.12%-Al(OH)(1,4-NDC)@4-ZIF-67 (line h).

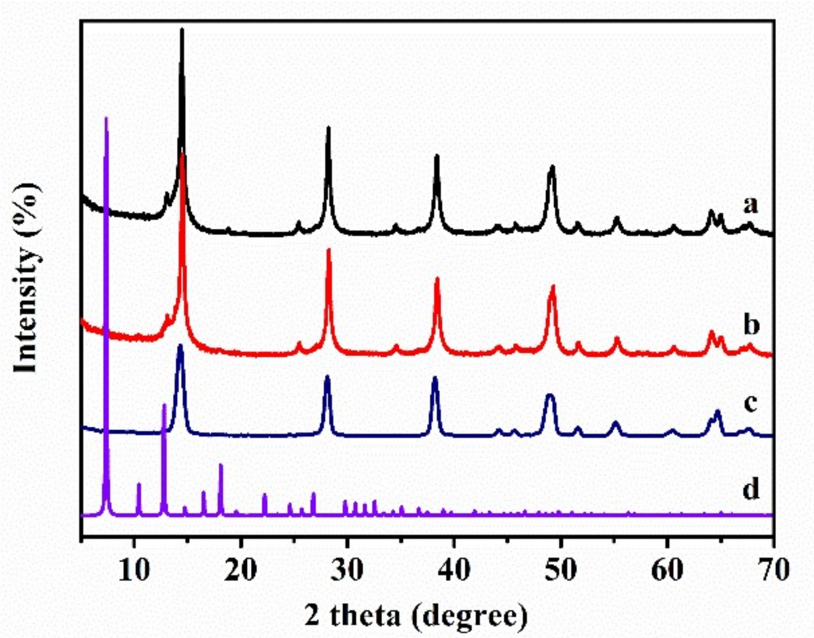

Fig. S7 XRD patterns of γ-AlOOH@2-ZIF-67 (line a); γ-AlOOH@4-ZIF-67 (line b); γ-AlOOH (line c); ZIF-67 (line d).

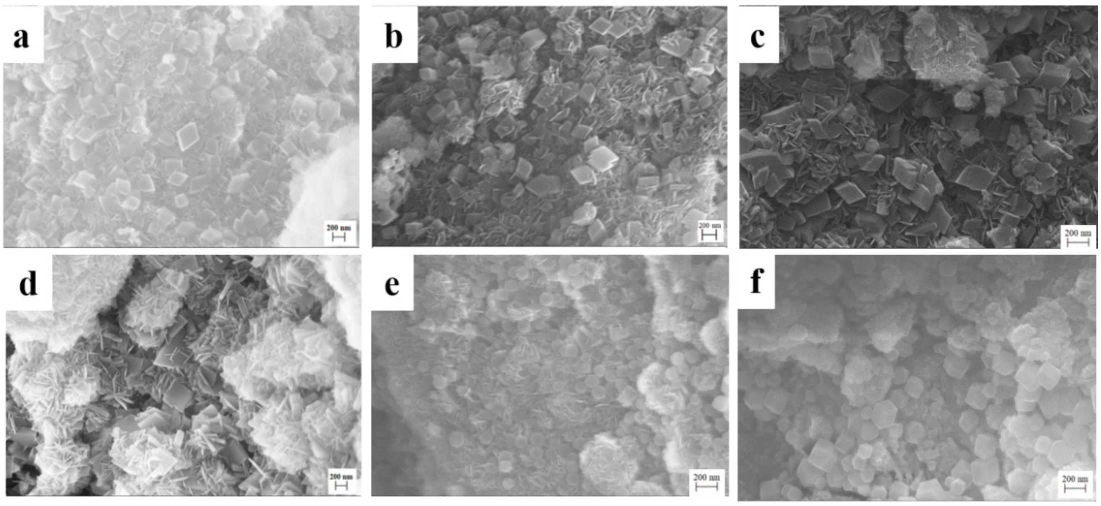

Fig. S8 SEM patterns of γ-AlOOH(a), γ-AlOOH@1.02%-Al(OH)(1,4-NDC) (b), γ-AlOOH@1.12%-Al(OH)(1,4-NDC) (c), γ-AlOOH@2.61%-Al(OH)(1,4-NDC) (d), γ-AlOOH@1.12%-Al(OH)(1,4-NDC)@2-ZIF-67 (e),γ-AlOOH@1.12%-Al(OH)(1,4-NDC)@4-ZIF-67 (f).

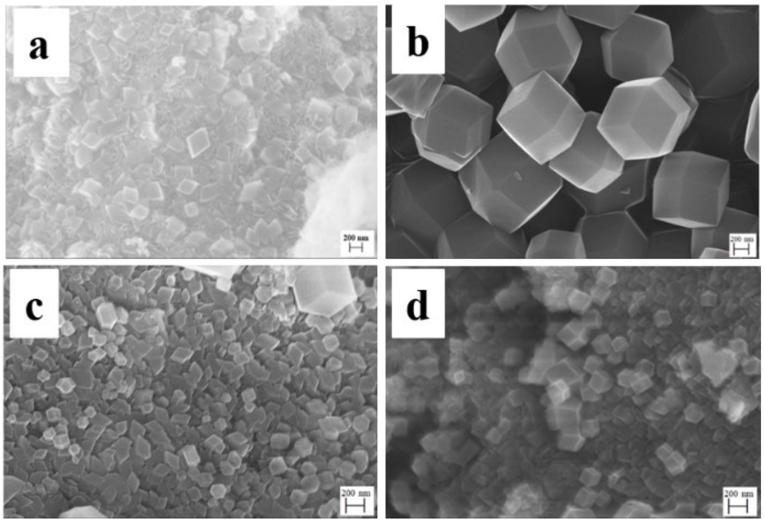

Fig. S9 SEM patterns of γ-AlOOH (a), ZIF-67(b), γ-AlOOH@2-ZIF-67 (c), γ-AlOOH@4-ZIF-67 (d).

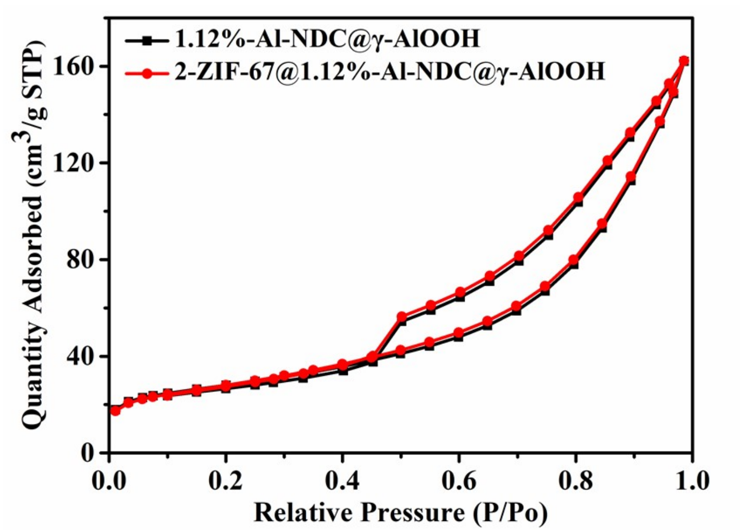

Fig. S10 The N_2 Adsorption-desorption isotherms of γ-AlOOH@1.12%-Al(OH)(1,4-NDC) and γ-AlOOH@1.12%-Al(OH)(1,4-NDC)@2-ZIF-67.

Table S1 BET characterization data for chromatographic stationary phase materials.

Chromatographic stationary phase	Specific surface area (m^2/g)	Pore volume (cm^3/g)	Average aperture (nm)
γ-Al_2O_3	205.2	0.484	7.64
γ-AlOOH	294.30	0.69	8.49
γ-AlOOH@1.12%-Al(OH)(1,4-NDC)	97.75	0.2435	10.86
γ-AlOOH@1.12%-Al(OH)(1,4-NDC)@2-ZIF-67	99.39	0.2471	10.12
γ-AlOOH@2-ZIF-67	78.37	0.2175	11.59

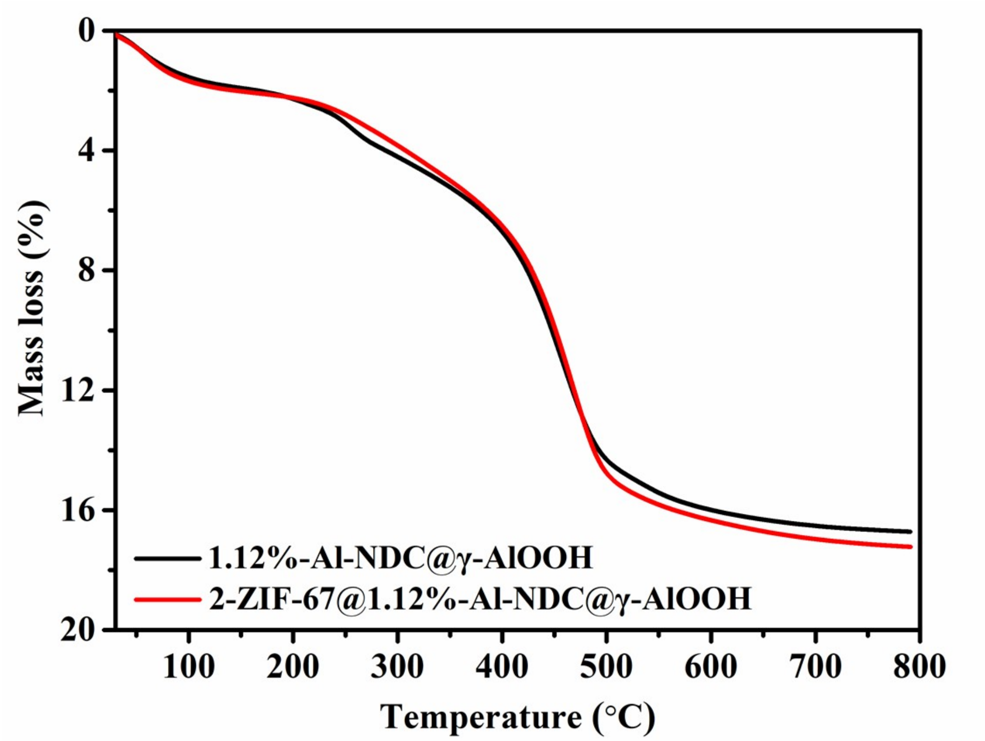

Fig. S11 Thermogravimetric curves of composites γ-AlOOH@1.12%-Al(OH)(1,4-NDC) and γ-AlOOH@1.12%-Al(OH)(1,4-NDC)@2-ZIF-67.

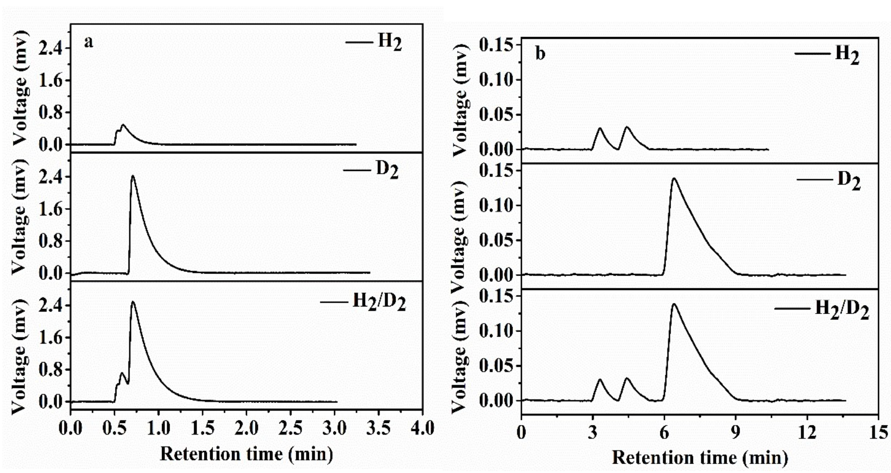

Fig. S12 The chromatograms of H_2, D_2 and the H_2/D_2 gas mixture over γ-AlOOH (a) and γ-AlOOH@1.12%-Al(OH)(1,4-NDC) (b) as a stationary phase, respectively. (Chromatographic conditions: Column temperature, 77 K; Injection volume: 125 μL for H_2, 125 μL for D_2 and 250 μL H_2/D_2 gas mixture (V_{H2}:V_{D2} = 1:1); Carrier gas He flow rate, 90 mL/min).

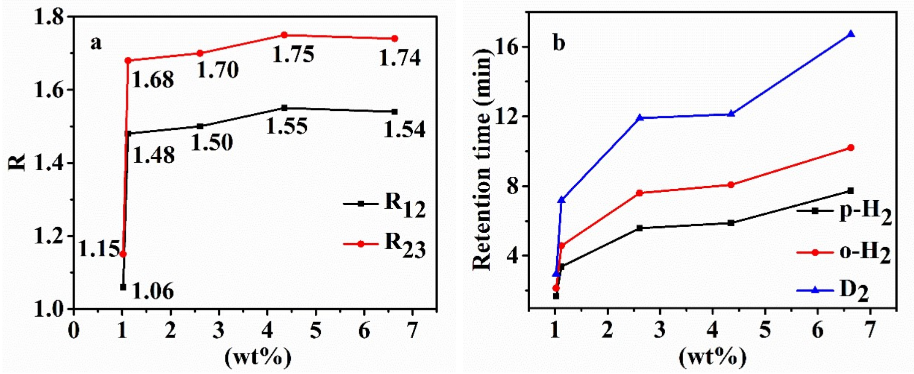

Fig. S13 The relationship between the content of Al(OH)(1,4-NDC) in γ-AlOOH@m-Al(OH)(1,4-NDC) (m = 1.02%, 1.12%, 2.61%, 4.35%, 6.63%) and the resolution (a), and the retention time (b) to separate H_2/D_2. Chromatographic conditions: column temperature, 77 K; injection volume of H_2/D_2 mixture, 50 μL H_2/D_2 gas mixture(V:V= 1:1); carrier gas He flow rate, 30 ml·min^{-1}.

The theoretical plate number and the corresponding height equivalent to a theoretical plate (HETP) calculated using the formula (S1) and (S2),

$$\text{theoretical plate number} = 5.54(t_R/w_{1/2})^2 \quad (S1)$$

$$\text{HETP} = L/\text{theoretical plate number} \quad (S2)$$

where L is the column length, t_R is the retention time and $W_{1/2}$ is the half-width.

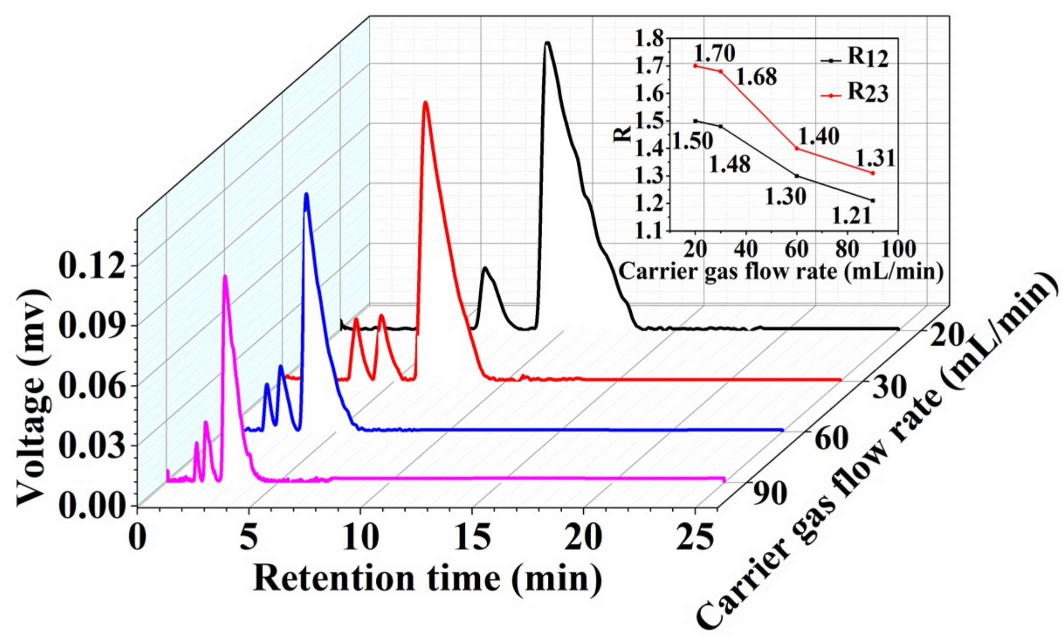

Fig. S14 Separation chromatogram of H_2/D_2 with γ-AlOOH@1.12%-Al(OH)(1,4-NDC) as chromatographic stationary phase under different carrier gas flow rates (inset: relationship between carrier gas flow rate and resolution). Chromatographic separation conditions: Column temperature, 77 K; Injection volume, 50 μL; Carrier gas flow rate of He, 20, 30, 60, 90 mL·min^{-1}).

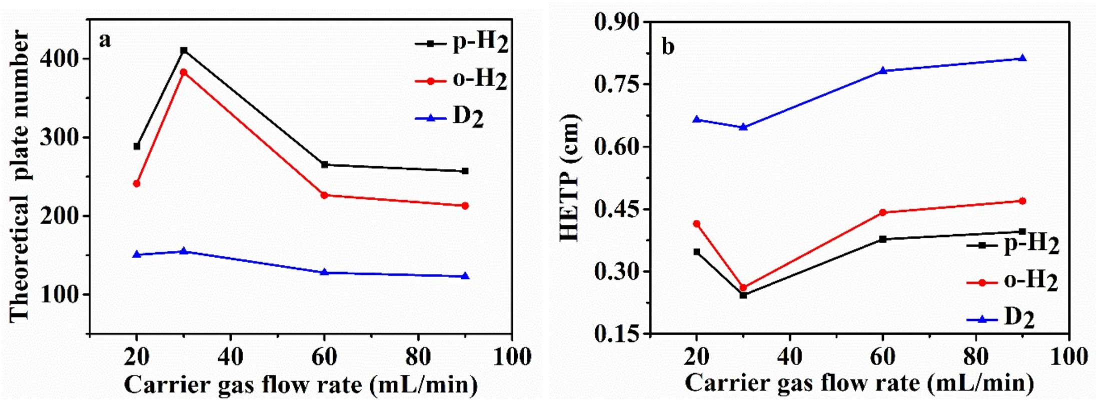

Fig. S15 The relationship between carrier gas flow rate and the number of theoretical plate (a) or the HETP (b) with γ-AlOOH@1.12%-Al(OH)(1,4-NDC). Chromatographic separation conditions: Column temperature, 77 K; Injection volume, 50 μL; Carrier gas flow rate of He, 20, 30, 60, 90 mL·min^{-1}.

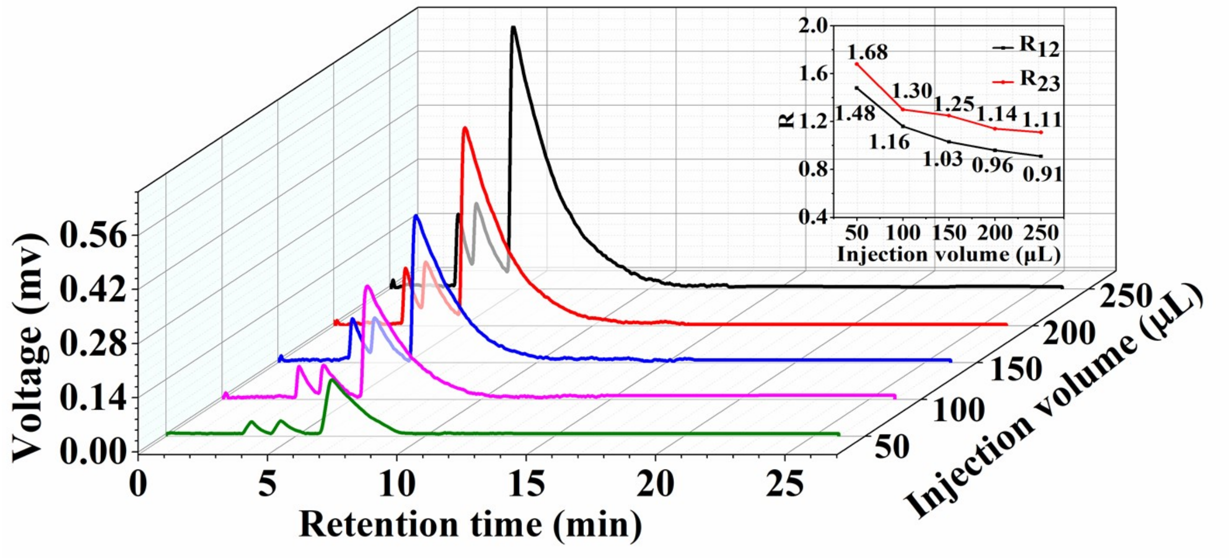

Fig. S16 Separation Chromatography of H_2/D_2 with different injection quantities using γ-AlOOH@1.12%-Al(OH)(1,4-NDC) as stationary phase (inset: the relationship between resolution and injection volume). (Chromatographic separation conditions: Column temperature, 77 K; Injection volume, 50, 100, 150, 200, 250 μL; Carrier gas He flow rate, 30 mL·min^{-1}).

Table S2 Parameters of γ-AlOOH@1.12%-Al(OH)(1,4-NDC)@n-ZIF-67 (n = 0, 1, 2, 3, 4), H_2 and D_2 for different ZIF-67 loading cycles at 77 K with gas flow rate 30 mL·min^{-1} and H_2/D_2 mixture injection volume 50 μL (V_{H2}:V_{D2} = 1:1).

Materials	Load number of ZIF-67 (n)	Retention time (t_R, min)		R	Separation time (min)
		H_2	D_2		
γ-AlOOH@1.12%-Al(OH)(1,4-NDC)@n-ZIF-67	0	3.40 4.67	7.26	1.48 1.68	10.36
	1	3.78	6.38	1.99	8.54
	2	3.27	5.42	2.02	7.72
	3	4.26	6.78	2.04	9.43
	4	4.63	7.71	2.07	10.43

Table S3 Parameters of γ-AlOOH@1.12%-Al(OH)(1,4-NDC)@2-ZIF-67 to separate H_2 and D_2 for different carrier gas flow rate at 77 K with H_2/D_2 mixture injection volume 50 μL (V_{H2}:V_{D2} = 1:1).

Material	Carrier flow rate (mL/min)	Retention time (t_R, min)		R	Separation time (min)
		H_2	D_2		
γ-AlOOH@1.12%-Al(OH)(1,4-NDC)@2-ZIF-67	20	4.52	8.10	2.05	10.90
	30	3.27	5.42	2.02	7.72
	60	1.78	2.97	1.99	4.38
	90	1.30	2.15	1.83	2.98
	120	0.95	1.53	1.63	2.10

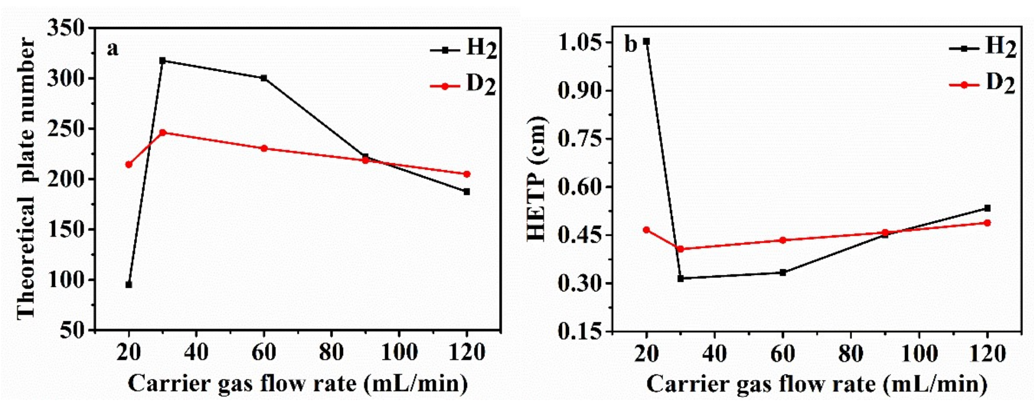

Fig. S17 The relationship between carrier gas flow rate and the theoretical plate number (a) and the height equivalent of theoretical plates (b) by γ-AlOOH@1.12%-Al(OH)(1,4-NDC)@2-ZIF-67**.** Chromatographic separation conditions: Column temperature, 77 K; H_2/D_2 mixture injection volume, 50 μL (V_{H2}:V_{D2} = 1:1); Carrier gas He flow rate, 120,90, 60, 30, 20 mL·min^{-1}.

Table S4 Parameters of H_2/D_2 mixture ($V_{H2}:V_{D2}$ = 1:1) separation at 77 K by γ-AlOOH@1.12%-Al(OH)(1,4-NDC)@2-ZIF-67 with carrier gas He flow rate 30 mL·min^{-1}

Sampling volume (μL)	Peak Height (mV)		Peak area (mV·min)		R	Separation time (min)
	H_2	D_2	H_2	D_2		
50	112.41	282.91	2827.55	15145.00	2.02	7.72
100	207.65	541.19	6040.40	30671.70	1.72	8.12
150	272.95	724.44	7953.40	44657.20	1.65	8.21
200	365.31	957.57	10330.30	57458.31	1.58	8.02
250	442.68	1180.41	12963.65	70540.31	1.56	7.74

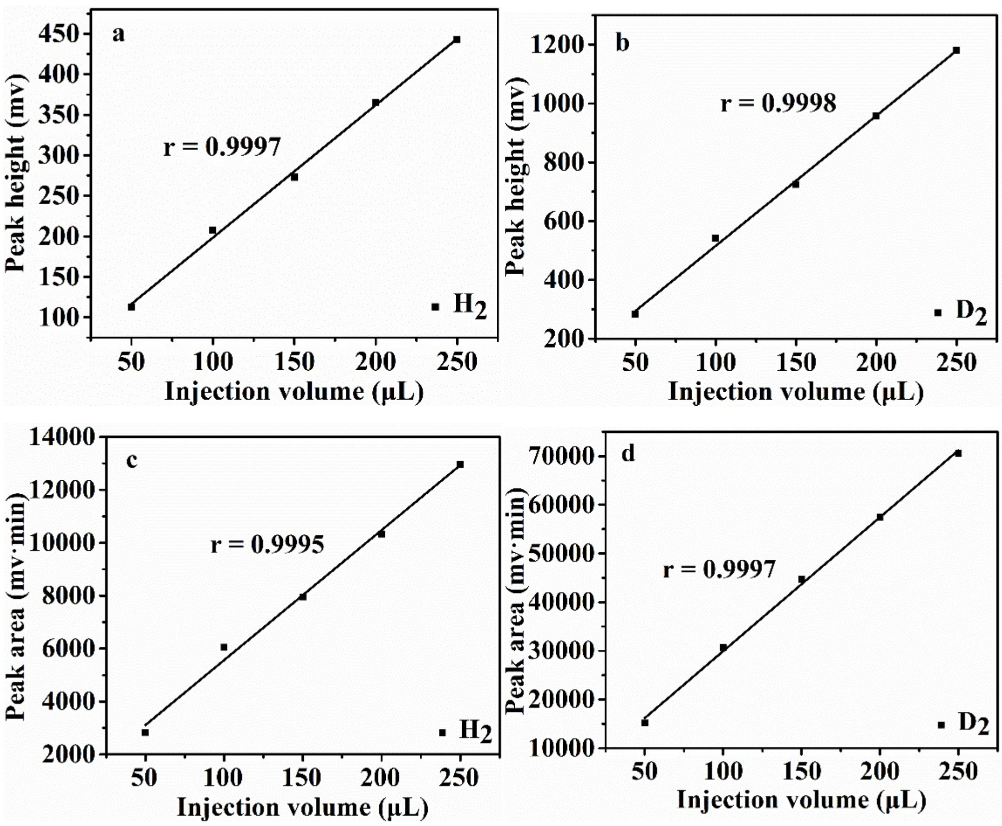

Fig. S18 The relationship between the injection volume of H_2 and D_2 in the H_2/D_2 mixture ($V_{H2}:V_{D2}$ = 1:1) with peak height of H_2 (a) and D_2 (b) , and the peak area of H_2 (c) and D_2 (d).

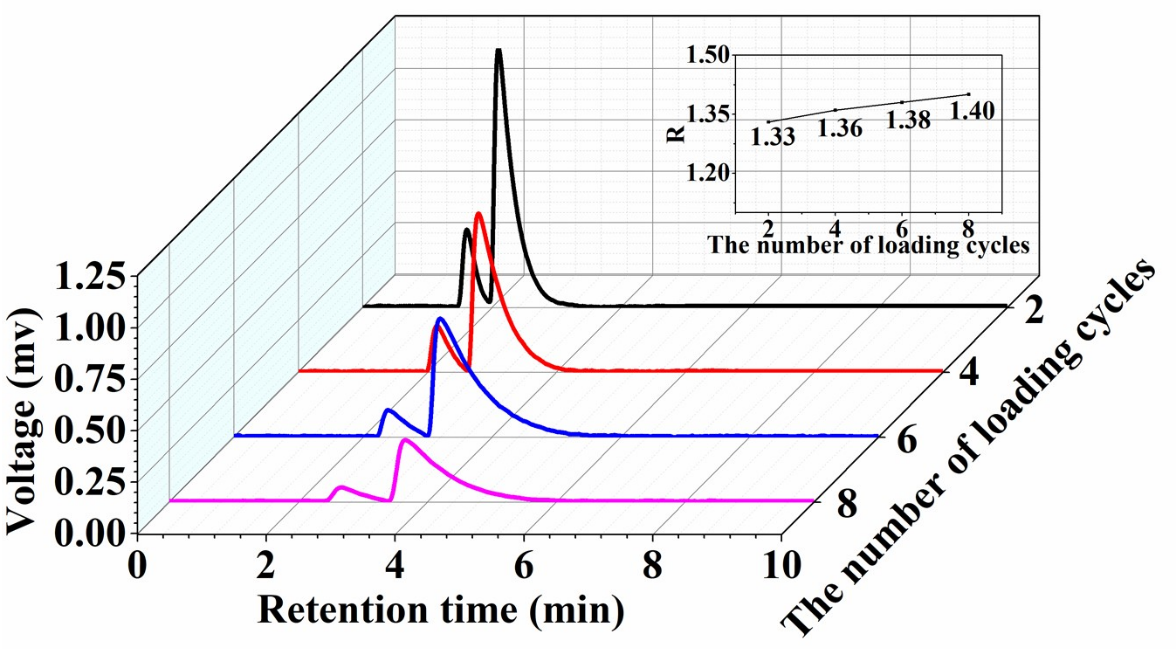

Fig. S19 Chromatograms of H_2/D_2 with γ-AlOOH@n'-ZIF-67 (n' = 2, 4, 6, 8) as chromatographic stationary phase. Chromatographic separation conditions: Column temperature, 77 K; H_2/D_2 mixed gas injection volume, 50 μL; Carrier gas He flow rate, 20 mL·min^{-1}.

Table S5 Parameters of γ-AlOOH@n-ZIF-67, H_2 and D_2 for different ZIF-67 loading cycles with H_2/D_2 mixture injection volume 50 μL (V_{H2}:V_{D2} = 1:1)

	ZIF-67 load number (n)	Retention time (min)		R	Separation time (min)
		H_2	D_2		
Materials	2	1.68	2.25	1.33	3.64
	4	2.31	3.04	1.35	4.60
	6	2.65	3.61	1.38	5.54
	8	2.92	4.10	1.42	6.60

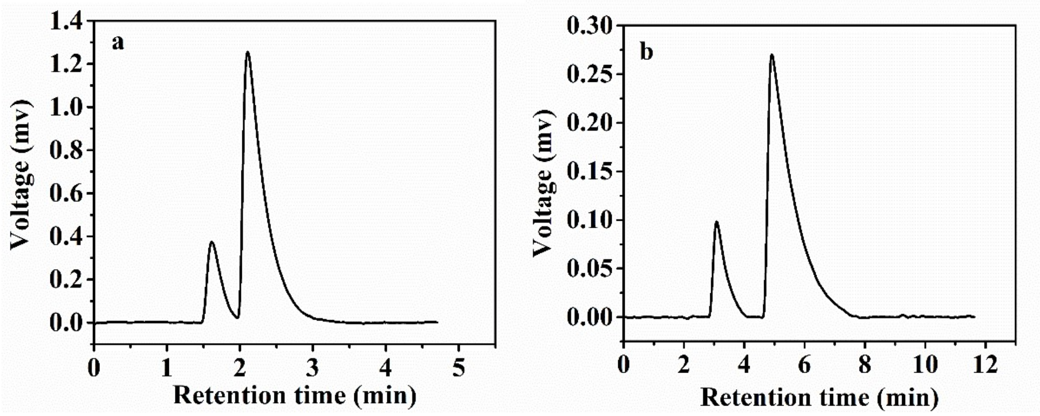

Fig. S20 Chromatograms of H_2/D_2 separation with γ-AlOOH@1.12%-Al(OH)(1,4-NDC)@2-ZIF-67 (a) and γ-AlOOH@2-ZIF-67 (b) as chromatographic stationary phases. Chromatographic separation conditions: Column temperature, 77 K; Injection volume, 50 μL; Carrier gas He flow rate a: 30 mL·min^{-1}, b: 20 mL·min^{-1}.

Table S6 Reproducibility of retention time, peak height and peak area of pure H_2 and pure D_2, and the corresponding relative standard deviation (RSD) percentage with γ-AlOOH@1.12%-Al(OH)(1,4-NDC)@2-ZIF-67 as chromatographic stationary phase.

Test times	H_2			D_2		
	Retention time (min)	Peak Height (mV)	Peak area (mV·min)	Retention time (min)	Peak height (mV)	Peak area (mV·min)
1	3.097	173.217	6231.100	4.883	516.908	38376.852
2	3.048	174.121	6257.500	4.833	490.255	35665.500
3	3.020	169.060	6081.950	4.898	491.063	33461.699
4	3.025	156.372	5913.700	4.865	494.811	34644.148
5	3.032	179.000	6005.800	4.797	495.389	34828.949
6	3.050	173.994	6372.600	4.757	503.047	35697.652
7	3.027	177.159	5931.700	4.862	516.835	34463.500
8	2.992	183.184	6304.700	4.840	524.825	36018.000
9	3.012	180.320	5993.800	4.772	518.782	32798.098
10	3.048	178.456	5824.100	4.830	533.649	36452.848
Average	3.035	174.488	6091.695	4.834	508.556	35240.725
SD	0.028	7.546	187.720	0.046	15.531	1583.204
RSD (%)	0.923	4.325	3.082	0.952	3.054	4.493

Table S7 Reproducibility of H_2/D_2 mixture (25 μL:25 μL) isotope separation and the corresponding standard deviation (SD), relative standard deviation percentage (%RSD), relative deviation percentage (%) under optimal conditions with γ-AlOOH@1.12%-Al(OH)(1,4-NDC)@2-ZIF-67 as chromatographic stationary phase.

Test times	Retention time (min)		Peak Area (SD_{H2} and SD_{D2}) of components in mixed samples (mV·min)		Content determined（%）		Relative deviation（%）	
	H_2	D_2	H_2	D_2	H_2	D_2	H_2	D_2
1	3.228	5.140	2901.500	17145.600	47.630	48.650	-4.74	-2.70
2	3.220	5.138	3027.200	16669.051	49.690	47.300	-0.62	-5.40
3	3.217	5.095	2835.150	16283.601	46.540	46.210	-6.92	-7.58
4	3.182	5.000	3035.400	16258.601	49.830	46.140	-0.34	-7.72
5	3.155	4.962	2862.200	16327.100	46.990	46.330	-6.02	-7.34
6	3.147	4.882	2919.000	16687.100	47.920	47.350	-4.16	-5.30
7	3.100	4.888	3028.550	16846.500	49.720	47.800	-0.56	-4.40
8	3.072	4.828	2748.600	16990.500	45.120	48.210	-9.76	-3.58
9	3.047	4.750	2826.800	16286.700	46.400	46.220	-7.20	-7.56
10	3.017	5.032	2842.000	17042.100	46.650	48.360	-6.70	-3.28
Ave.	3.139	4.972	2902.640	16653.685	47.649	47.257	-4.70	-5.49
SD	0.076	0.134	99.225	346.284	1.630	0.980	/	/
RSD(%)	2.421	2.695	3.418	2.079	3.421	2.074	/	/